

A New Equation of Load Curve of Critical Wrinkles Variable Blank Holder Force in the Warm Deep-Drawing of Twin-Roll Cast Mg Sheets

Zhimin Liu, Shuming Xing, Peiwei Bao, Lingyun Zhao, Desen Yang, Shuping He, Lijun Chen, Yuangang Deng and Xiangju Yuan

Abstract A new equation of load curve of critical wrinkles variable blank holder force (VBHF) during the warm deep-drawing of twin-roll cast Mg sheets was derived, which based on correlative energy conservation theorem. Experiments of limited drawing ratio (LDR) suggested that calculated load curve of minimum wrinkles using the new formulas fit to the tested data very well. The LDR was improved from 1.75 to 1.92 by using a new three segments way of load VBHF applied in the warm deep-drawing, at the forming temperature of 523 K and punch velocity of 45 mm/min. Finally, the VBHF warm deep-drawing process is also simulated by the finite element method, and a new technique of variable punch velocity (VPV) is applied in the simulation. The simulation indicated that the VPV technology can improve the LDR from 1.86 to 2.26 and gain the whole cylinder part, at the forming temperature of 523 K, when the punch velocity varied gradually from 30 to 5 mm/s.

Keywords Magnesium alloy · Twin-roll cast · Blank holder force · Warm deep-drawing · Limit drawing ratio

F2012-H01-002

Z. Liu (✉) · L. Zhao · D. Yang · S. He · L. Chen · Y. Deng · X. Yuan
Institute of Stamping Design, Department of Process, Changan Automobile Co., Ltd,
401120 Chongqing, China
e-mail: 007liuzhimin@163.com

S. Xing · P. Bao
School of Mechanical, Electronic and Control Engineering, Beijing Jiaotong University,
100044 Beijing, China
e-mail: shumingxing1962@126.com

1 Introduction

As the lightest structural material, magnesium alloys have high potential application in automobile body manufacture [1–3]. However, the poor formability at room temperature make the stamping part of the magnesium alloy sheet must be formed at high temperature [4, 5]. The stamping technique of variable blank holder force (VBHF) was the effective way to improve the formability of sheet, forming precision and surface quality [6, 7]. In recent years, how to implement the VBHF technology has become one of the research emphases in the field of sheet metal forming [8, 9]. Generally, the load curve of minimum wrinkles were usually calculated by the equation of blank holder force (BHF) based on the Fields-Backofen model. Nevertheless, magnesium alloys usually generated easily the conspicuous dynamic recrystallization during high temperature deformation, which resulted in the sharp soften phenomena. So the equation of BHF based on the Fields-Backofen model can not fit to the deep-drawing of magnesium sheets.

Therefore, the aim of the present investigation is to propose a VBHF engineering equation of the curve of minimum wrinkles suit for the magnesium alloy sheet, optimize and control the BHF during the process of deep-drawing. In this research, based on the plastic theory and consulting correlative energy conservation theorem, a new theoretical mathematic models of BHF had been established during the process of deep drawing, which including the factors of the characteristics of magnesium alloy material at the high temperature and the structure of stamping dies. Experiments of limited drawing ratio (LDR) at warm temperature are performed to validate the new equation of variable BHF. Finally, the VBHF technology is discussed by the numerical approach.

2 Equation Derivation

According to the correlative energy conversation theorem, the released energy of single ripple U_θ can be described as follows [10, 11]:

$$U_\theta = U_w + U_Q \quad (1)$$

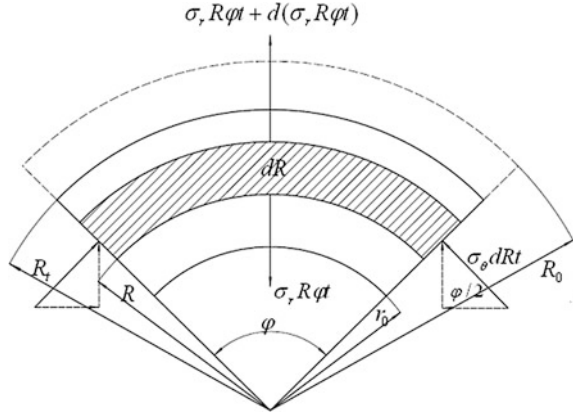
where U_w is the required bending work, and U_Q is the wasting work of the BHF.

The external force act on the differential bulk of the sheet during arbitrary stage of deep-drawing is illustrated in Fig. 1. Where the radius of flange R_0 change to R , φ is the central angle of arbitrary arc, dR is the width of fan-shaped bulk, t is the thickness, σ_θ is tangent stress, σ_r is radial stress.

When the external force acted on the differential bulk is on balance, the radial force can be described as follows:

$$\sigma_r R \varphi t + d(\sigma_r R \varphi t) - \sigma_r R \varphi t + 2\sigma_\theta dR t \sin \frac{\varphi}{2} = 0 \quad (2)$$

Fig. 1 The differential bulk of the sheet



When the angle ϕ is wee, variable the thickness can be ignored, i.e. $dt = 0$, Eq. (2) can be written as:

$$d\sigma_r = -(\sigma_r + \sigma_\theta) \frac{dR}{R} \quad (3)$$

The surface ripple of the flange can be shown in Fig. 2, and the mathematical model of the wrinkle can be described as:

$$y = \frac{y_0}{2} \left(1 - \cos 2\pi \frac{\phi}{\phi_0} \right) \left(\frac{R-r}{R_t-r} \right)^{1/2} \quad (4)$$

where R_t is the external radius of flange, r is the internal radius of flange, R is the radius of arbitrary point in the flange, ϕ_0 is the central angle, ϕ is the central angle of arbitrary arc, y_0 is the maximum flexibility of single ripple, y is the flexibility of arbitrary point in the flange.

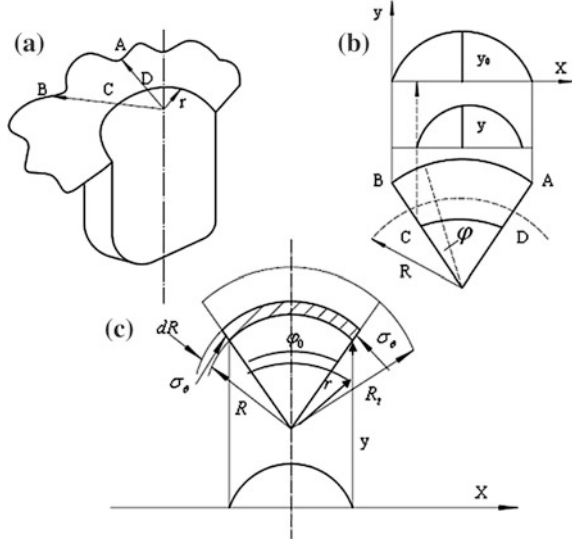
As our former research about characteristics of twin-roll cast *Mg* sheets [12, 13], the dislocation glide is dominant deformation mechanisms at high temperature and lower strain rate, i.e. $Z < Z_0$. So the equation of stress-strain curve can be written as [13]:

$$\begin{aligned} \sigma_i &= K_1 \cdot [\sigma_{ss}^{*2} + (\sigma_0^2 - \sigma_{ss}^{*2}) \cdot \exp(-\Omega \varepsilon_i)]^{0.5} + K_2 \cdot \exp(\varepsilon_i/\varepsilon_0) \\ &= K_1 \cdot [A + B \exp(-\Omega \varepsilon_i)]^{0.5} + K_2 \cdot \exp(\varepsilon_i/\varepsilon_0) \end{aligned} \quad (5)$$

where Ω is a constant reflecting dislocation annihilation and rearrangement, σ_0 is the initial stress, and σ_{ss}^* is the saturation stress.

Since the flange is in the stage of plane stress, according to the Eqs. (3) and (5), the radial stress σ_r can be derived as:

Fig. 2 The surface ripple of the flange



$$\sigma_r = -K_1 \int \left\{ A + B \exp \left[-\frac{\Omega R_t}{R} \left(1 - \frac{R_t}{R_0} \right) \right] \right\}^{0.5} \cdot \frac{dR}{R} - K_2 \int \exp \left[\frac{R_t}{\varepsilon_0 R} \left(1 - \frac{R_t}{R_0} \right) \right] \cdot \frac{dR}{R} \quad (6)$$

Similarly, the tangent stress σ_θ can be given as follows:

$$\sigma_\theta = K_1 \left[A + B \exp \left(-\frac{M}{R} \right) \right]^{0.5} + K_2 \exp \left(\frac{N}{R} \right) + K_1 \int \left[A + B \exp \left(-\frac{M}{R} \right) \right]^{0.5} \cdot \frac{dR}{R} + K_2 \int \exp \left(\frac{N}{R} \right) \cdot \frac{dR}{R} = \left\{ K_1 \left[A + B \exp \left(-\frac{M}{R} \right) \right]^{0.5} + K_1 \sigma_d \right\} + \left\{ K_2 \exp \left(\frac{N}{R} \right) + K_2 \sigma_{sem} \right\} \quad (7)$$

where assume $M = \Omega R_t \left(1 - \frac{R_t}{R_0} \right)$, $N = \frac{R_t}{\varepsilon_0} \left(1 - \frac{R_t}{R_0} \right)$, $\sigma_{sem} = \int \exp \left(\frac{N}{R} \right) \cdot \frac{dR}{R}$,

$\sigma_d = \int \left[A + B \exp \left(-\frac{M}{R} \right) \right]^{0.5} \cdot \frac{dR}{R}$.

Based on the mathematical of the wrinkle [10], according to Eq. (7) the energy U_θ can be expressed as:

$$U_\theta = \int_r^R \sigma_\theta S' t dR = \frac{1}{2} \int_r^{R_t} \int_0^{\phi_0} \frac{\pi^2 y_0^2}{\phi_0^2} \frac{1}{R} \frac{R-r}{R_t-r} \sin^2 \frac{2\pi\phi}{\phi_0} \cdot \left\{ K_1 \left[A + B \exp \left(-\frac{M}{R} \right) \right]^{0.5} + K_1 \sigma_d + K_2 \exp \left(\frac{N}{R} \right) + K_2 \sigma_{sem} \right\} t d\phi dR \quad (8)$$

Likewise, in stage of the plane stress the required bending work U_w can be derived as:

$$\begin{aligned}
 U_w &= \int_r^{R_t} \int_0^l \frac{1}{2} D \left(\frac{d^2 y}{dx^2} \right)^2 dldx = \int_r^{R_t} \int_0^l \frac{1}{2} \frac{d\sigma_i}{d\varepsilon_0} \left(\frac{d^2 y}{dx^2} \right)^2 dldx \\
 &= \frac{\pi^4 y_0^2 t^3}{6\phi_0^4 (R_t - r)} \int_r^{R_t} \int_0^{\phi_0} \frac{R - r}{R^3} \cos^2 \left(\frac{2\pi\phi}{\phi_0} \right) \cdot \left[-\frac{B\Omega K_1 \exp\left(-\frac{M}{R}\right)}{2\sqrt{A + B \exp\left(-\frac{M}{R}\right)}} + \frac{K_2}{\varepsilon_0} \exp\left(\frac{N}{R}\right) \right] d\phi dR
 \end{aligned} \quad (9)$$

The blank holder force Q can be given by [10]:

$$Q = \frac{2\pi}{y_0 \phi_0} (U_\theta - U_w) = \frac{2\pi}{y_0} \left(\frac{U_\theta}{\phi_0} - \frac{U_w}{\phi_0} \right) \quad (10)$$

where ϕ_0 is the central angle of arbitrary ripple, y_0 is the maximum flexibility at the location of $R = R_t$ on the flange.

Substituting Eqs. (8)–(9) into Eq. (10), and the differential coefficient equation of blank holder force Q can be written as:

$$\frac{\partial Q}{\partial \phi_0} = \frac{\pi^2 y_0^2 t^3 V}{4(R_t - r)} \cdot \frac{1}{\phi_0^2} + \left[\frac{\pi^4 y_0^2 t^3}{24(R_t - r)} \left(\frac{2K_2}{\varepsilon_0} D_{sem} - B\Omega K_1 D_d \right) \right] \cdot \frac{1}{\phi_0^4} \quad (11)$$

where

$$\begin{aligned}
 V &\approx 2K_1 \sqrt{A}(r + M) \left[\exp\left(-\frac{M}{R_t}\right) - \exp\left(-\frac{M}{r}\right) \right] + 2K_2 (R_t - r) \\
 &\quad - \frac{3}{4} K_2 N^2 \left(\frac{1}{R_t} - \frac{1}{r} \right) - \left(\frac{1}{R_t^2} - \frac{1}{r^2} \right) \left(\frac{K_2 N^3}{12} + \frac{K_2 r N^2}{8} \right) - \left(\frac{1}{R_t^3} - \frac{1}{r^3} \right) \left(\frac{K_2 r N^3}{27} \right) \\
 &\quad + K_2 \ln\left(\frac{r}{R_t}\right) \cdot (r \ln N - 2N - r) + \frac{2K_1 \sqrt{A}}{M} \left[R_t \exp\left(-\frac{M}{R_t}\right) - r \exp\left(-\frac{M}{r}\right) \right] \\
 &\quad + \frac{2rK_1 \sqrt{A}}{M} \cdot \left[R_t \exp\left(-\frac{M}{R_t}\right) - r \exp\left(-\frac{M}{r}\right) + \frac{R_t}{M} \exp\left(-\frac{M}{R_t}\right) - \frac{r}{M} \exp\left(-\frac{M}{r}\right) \right] \\
 &\quad + K_2 \left[R_t \ln\left(\frac{N}{R_t}\right) - r \ln\left(\frac{N}{r}\right) \right] + \frac{K_2 r}{2} (\ln^2 R_t - \ln^2 r) \\
 D_d &\approx \frac{2\sqrt{A + B \exp\left(-\frac{M}{R_t}\right)}}{MB} \cdot \left(\frac{r}{R_t} - \frac{2r}{M} - 1 \right) - \frac{2\sqrt{A + B \exp\left(-\frac{M}{r}\right)}}{MB} \cdot \frac{2r}{M}
 \end{aligned}$$

$$D_{sem} = \frac{r}{N} \left[\frac{1}{R_t} \exp\left(\frac{N}{R_t}\right) - \frac{1}{r} \exp\left(\frac{N}{r}\right) \right] - \frac{1}{N} \left[\exp\left(\frac{N}{R_t}\right) - \exp\left(\frac{N}{r}\right) \right],$$

Then assumed the Eq. (11) equal to zero, i.e. $\frac{\partial Q}{\partial \phi_0} = 0$, the central angle ϕ_0 can be expressed in the form:

$$\phi_0 = \sqrt{\frac{\frac{\pi^4 y_0^2 t^3}{12(R_t - r)} \left(\frac{2K_2}{\varepsilon_0} D_{sem} - B\Omega K_1 D_d \right)}{\frac{\pi^2 y_0^2 t}{4(R_t - r)} V}} = \pi t \sqrt{\frac{1}{3V} \left(\frac{2K_2}{\varepsilon_0} D_{sem} - B\Omega K_1 D_d \right)} \quad (12)$$

Substituting Eq. (12) into (10), the variable BHF engineering equation of the curve of minimum ripple can be described as:

$$Q = \frac{3\pi}{4} \cdot \frac{y_0}{t(R_t - r)} \cdot \frac{\varepsilon_0 V^2}{2K_2 D_{sem} - B\Omega K_1 \varepsilon_0 D_d} \quad (13)$$

The Eq. (13) can be applied only on the given condition where the Zener-Hollomon parameter (Z) is less than the critical value Z_0 ($Z < 1.54E11$), and the dominant mechanism of TRC-Mg is slip.

When the Zener-Hollomon parameter (Z) is higher than the critical value Z_0 ($Z > 1.54E11$), consulting mechanism of the twinning, the equation of stress-strain curve can be described as follows [13]:

$$\sigma_i = K_1 X_T \sigma_{twin} + (1 - X_T) K_1 \cdot [A + B \exp(-\Omega \varepsilon_i)]^{0.5} + K_2 \cdot \exp(\varepsilon_i / \varepsilon_0) \quad (14)$$

where σ_{twin} is stress of twinning, X_T is the fraction of grains that have twinned, $\exp(\varepsilon_i / \varepsilon_0)$ is a breakage ratio function.

Since three types of mechanisms of the twinning, dislocation slip and semi-solid slip exist in the TRC magnesium sheet, the released energy of tangent stress U_θ can be written as:

$$U_\theta = [U_\theta]_{twin} + [U_\theta]_{slip} + [U_\theta]_{sem} \quad (15)$$

Similarly, in term of above derivation based on the mechanism of dislocation slip, the energy of tangent stress $[U_\theta]_{twin}$ can be given by:

$$[U_\theta]_{twin} = \frac{r X_T b K_1 \pi^2 y_0^2 t \left(1 - \frac{R_t}{R_0} \right)^n}{4n(R_t - r) \phi_0} \left\{ \frac{1}{n} \left[\left(\frac{R_t}{r} \right)^n - 1 \right] - \ln \left(\frac{R_t}{r} \right) \right\} + \frac{a K_1 X_T \pi^2 y_0^2 t}{4n(R_t - r) \phi_0} \left[(R_t - r) + R_t \ln R_t - r \ln r - (R_t - r) - \frac{r}{2} (\ln^2 R_t - \ln^2 r) \right] = K_\theta \cdot \frac{1}{\phi_0} \quad (16)$$

The summation energy of $[U_\theta]_{slip}$ and $[U_\theta]_{sem}$ can be described as:

$$[U_\theta]_{slip} + [U_\theta]_{sem} = \frac{\pi^2 y_0^2 t V'}{4(R_t - r) \phi_0} \quad (17)$$

where

$$\begin{aligned}
 V' \approx & 2K_1(1 - X_T)\sqrt{A}(r + M) \left[\exp\left(-\frac{M}{R_t}\right) - \exp\left(-\frac{M}{r}\right) \right] + 2K_2(R_t - r) \\
 & - \frac{3}{4}K_2N^2\left(\frac{1}{R_t} - \frac{1}{r}\right) - \left(\frac{1}{R_t^2} - \frac{1}{r^2}\right)\left(\frac{K_2N^3}{12} + \frac{K_2rN^2}{8}\right) - \left(\frac{1}{R_t^3} - \frac{1}{r^3}\right)\left(\frac{K_2rN^3}{27}\right) \\
 & + K_2 \ln\left(\frac{r}{R_t}\right) \cdot (r \ln N - 2N - r) \\
 & + \frac{2K_1(1 - X_T)\sqrt{A}}{M} \left[R_t \exp\left(-\frac{M}{R_t}\right) - r \exp\left(-\frac{M}{r}\right) \right] + \frac{2rK_1(1 - X_T)\sqrt{A}}{M} \\
 & \cdot \left[R_t \exp\left(-\frac{M}{R_t}\right) - r \exp\left(-\frac{M}{r}\right) + \frac{R_t}{M} \exp\left(-\frac{M}{R_t}\right) - \frac{r}{M} \exp\left(-\frac{M}{r}\right) \right] \\
 & + K_2 \left[R_t \ln\left(\frac{N}{R_t}\right) - r \ln\left(\frac{N}{r}\right) \right] + \frac{K_2r}{2} (\ln^2 R_t - \ln^2 r)
 \end{aligned}$$

In the same way, the required bending work $[U_w]_{twin}$ can be written as:

$$\begin{aligned}
 [U_w]_{twin} &= \frac{X_T b K_1 n t^3 \pi^4 y_0^2 \left(1 - \frac{R_t}{R_0}\right)^{n-1}}{12 R_t (R_t - r) \phi_0^3} \left\{ \frac{1}{n} \left[\left(\frac{R_t}{r}\right)^n - 1 \right] - \frac{r}{(1+n)R_t} \left[\left(\frac{R_t}{r}\right)^{n+1} - 1 \right] \right\} \\
 &= K_{w1} \cdot \frac{1}{\phi_0^3}
 \end{aligned} \tag{18}$$

The summation bending work of $[U_w]_{slip}$ and $[U_w]_{sem}$ can be written as:

$$\begin{aligned}
 [U_w]_{slip} + [U_w]_{sem} &= \left\{ \frac{\pi^4 y_0^2 t^3}{24(R_t - r)} \left[\frac{2K_2}{\varepsilon_0} D_{sem} - (1 - X_T) B \Omega K_1 D_d \right] \right\} \cdot \frac{1}{\phi_0^3} \\
 &= K_{w2} \cdot \frac{1}{\phi_0^3}
 \end{aligned} \tag{19}$$

So the variable BHF engineering equation of the curve of minimum wrinkles can be expressed as:

$$Q = \frac{\pi}{y_0} \left[\frac{48k_\theta^2(R_t - r)^2 + 24k_\theta(R_t - r)\pi^2 y_0^2 t V' + 3(\pi^2 y_0^2 t V')^2}{32(k_{w1} + k_{w2})(R_t - r)^2} \right] \tag{20}$$

In general, the variable BHF engineering equation of the curve of minimum wrinkles based on Fields-Backofen is given as [10, 11]:

$$Q = 1.5K \frac{y_0}{t} \cdot \frac{\pi r^2}{4} \cdot \frac{1}{n^3} (1 - \rho)^{1+n} \cdot \frac{\frac{\rho}{m} \left\{ \frac{1}{n} \left[\left(\frac{\rho}{m}\right)^n - 1 \right] - \ln \frac{\rho}{m} \right\}^2}{\left(\frac{\rho}{m} - 1\right) \left\{ \frac{1}{n} \left[\left(\frac{\rho}{m}\right)^n - 1 \right] - \frac{1}{1+n} \left[\left(\frac{\rho}{m}\right)^n - \frac{m}{\rho} \right] \right\}} \tag{21}$$

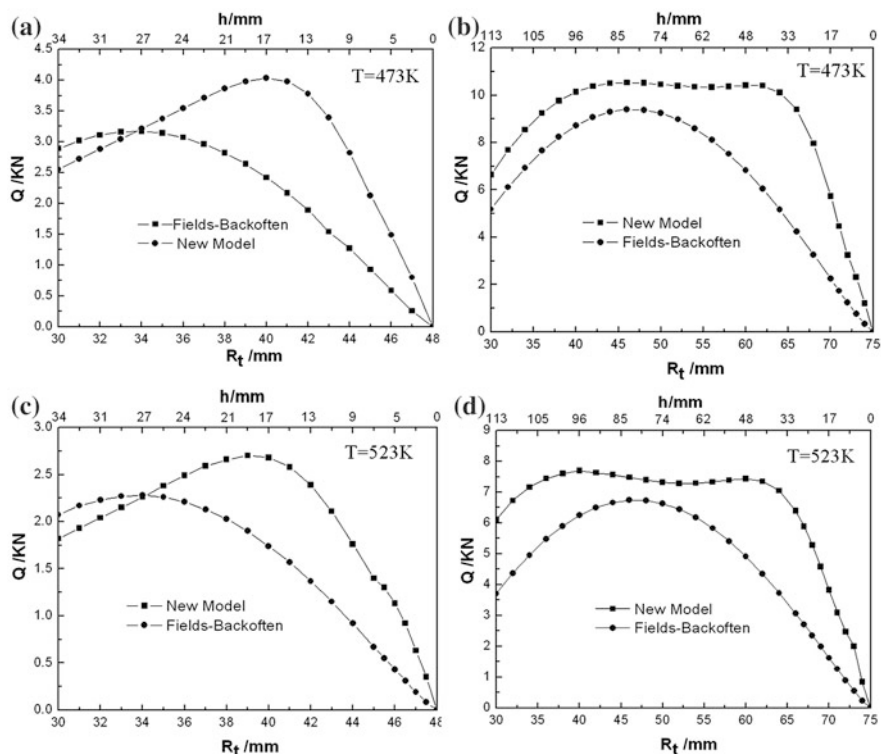


Fig. 3 The curves of minimum wrinkles BHF calculated by using two models

where K is the strength-hardening coefficient, n is the strain-hardening exponent, t is the sheet thickness, $\rho = R_t/R_0$ denotes the deep drawing phase and $m = r/R_0$ expresses the deep drawing ratio.

3 Application of the New Equation

The load curves of the minimum wrinkles VBHF of two magnesium sheets during the warm deep-drawing test were calculated, which based on the new model and Fields-Backofen respectively. Where the specimens are 3.3 mm thick, and the diameters are 96 and 150 mm respectively. The description of load curves of critical wrinkle in Fig. 3 illustrates that the peak of VBHF of the 96 mm diameter specimen calculated by using the new equation appears on the metaphase, but the peak of VBHF gained by using the Fields-Backofen occurs on the initial stage, when the temperature is less than 523 K. It can be clearly seen that the peak of VBHF of the 150 mm diameter gained by the new model have a platform, which corresponds to the influence between dynamic recrystallization and strain hardening during the warm deep-drawing.

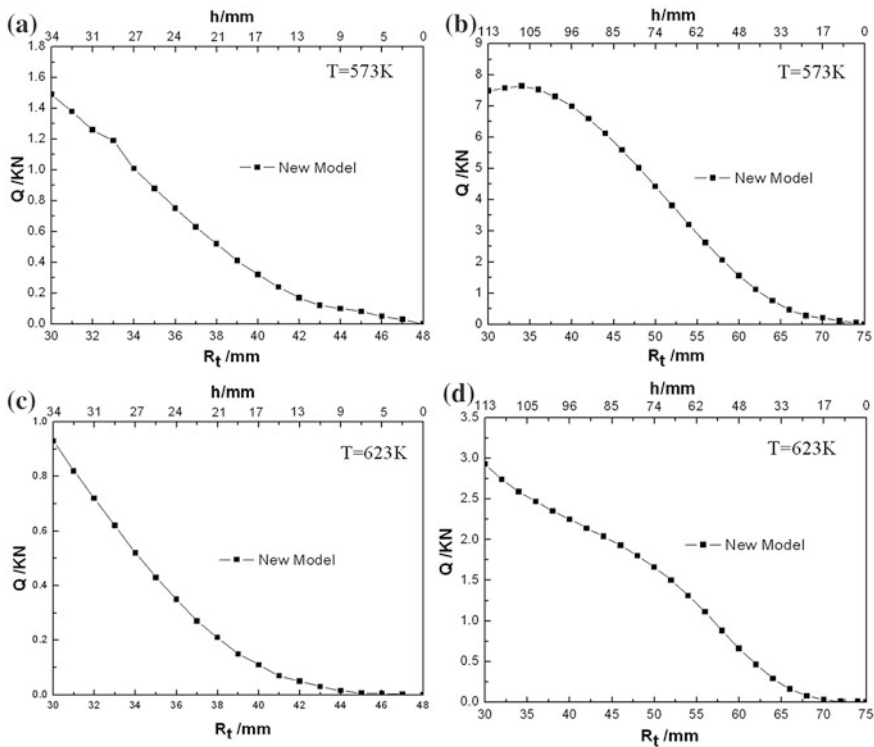


Fig. 4 The curves of minimum wrinkles BHF calculated by the new model

When the temperature is higher than 573 K, the load curves of the VBHF based on the new model were shown in Fig. 4, it can be seen that severe soften phenomena occur because of dynamic recrystallization. In addition, for the prominent dynamic recrystallization, the strength-hardening coefficient K and the strain-hardening exponent n can not be measured through hot tensile testing, which means the Fields-Backofen is not fit to the hot-stamping of magnesium alloy sheets.

In contrast, the peak values of VBHF were calculated and tested, as shown in Table 1. The different peak values of specimens during the warm deep-drawing testing reveal that the peak values calculated by using the new model fit to the experiment data very well, and the new model was more accurate than the Fields-Backofen model.

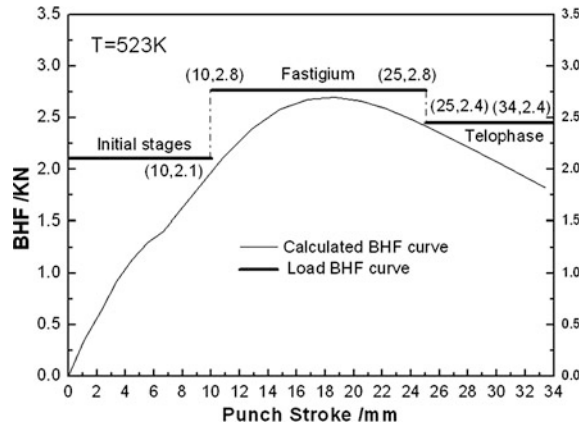
4 Numerical Studies of VBHF and Experiments

According to the theorem of VBHF in deep drawing, the designed load curve of critical wrinkles variable blank holder force should be similar to the calculated load curve. However, it is difficult to assure the blank holder force simultaneously

Table 1 Peak value of VBHF calculated by two models

Types of model	Diameter of sheet R/mm	Peak value	Peak value	Peak value	Peak value
		Q(T = 473 K)/KN	Q(T = 523 K)/KN	Q(T = 573 K)/KN	Q(T = 623 K)/KN
Fields-backofen model	48	3.07	2.28	—	—
	75	9.4	6.74	—	—
The new model	48	4.03	2.7	1.49	0.93
	75	10.39	7.7	7.3	2.93
Testing data	48	3.96	2.97	1.98	—
	75	9.9	7.92	6.93	—

Fig. 5 Punch load and calculated BHF curve by new model



change with the punch motion for the common equipment. So the three segments way of load VBHF was proposed during the warm deep-drawing according to the practical working-condition, as shown in Fig. 5. It is evident that the loading BHF have been optimize three stages, which are initial stages, fastigium and telophase. Comparison with the warm deep drawing experiments aided by the three segments way of VBHF and constant BHF, the results indicated that the limit drawing ratio (LDR) was improved from 1.75 to 1.92, when the forming temperature is 523 K and punch velocity is 45 mm/min.

The results of numerical simulation FLD revealed that LDR of constant BHF is 1.73, as shown in the Fig. 6a, and the LDR of the three segments way of VBHF can reach 1.86, as shown in Fig. 6b. Where the forming temperature is 532 K and the punch velocity is 30 mm/s.

Generally, magnesium alloys formability increase with decrease strain-rates. However, the lower strain-rates affect the efficiency of manufacture. So according to the practical working-efficiency, a new deep-drawing process through the approach of variable punch velocity (VPV) applied in the numerical simulation with using three segment way of VBHF, as described in Fig. 7. Where the forming temperature is 532 K and the punch velocity varies from 5 to 30 mm/s. It can be seen obviously that the LDR has been increased from 1.86 to 2.26, and gained the whole cylinder part. The new technique of VBHF combined VPV can be named

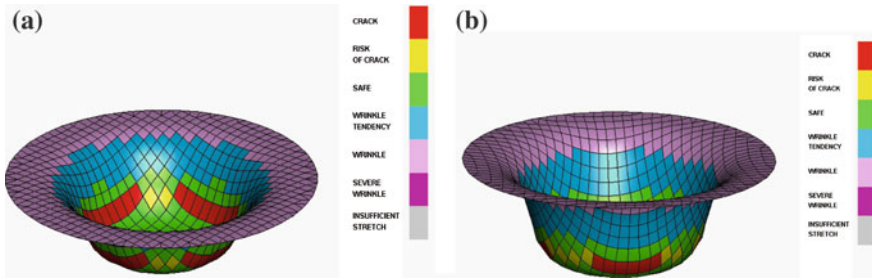


Fig. 6 Comparison of LDR with constant BHF and VBHF. **a** BHF, **b** VBHF

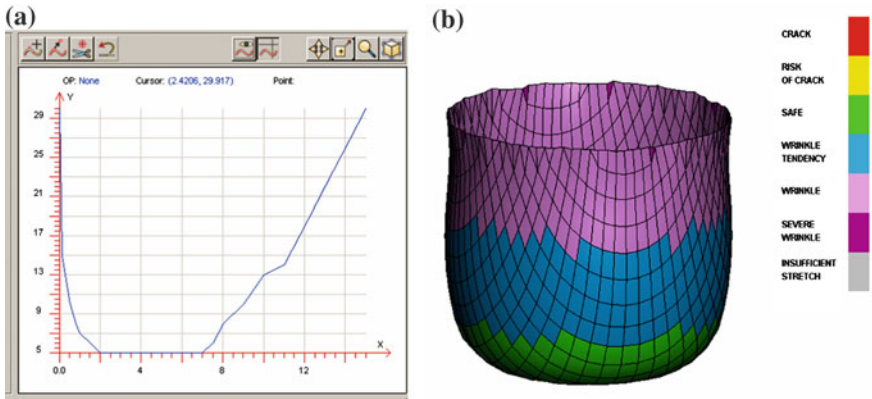


Fig. 7 The FLD of three segments way of VBHF combined VPV. **a** VPV, **b** FLD

servo-flexible stamping, which utilized to implement the VBHF simultaneously with VPV and stepwise motion.

Recently, several press builders developed metal forming presses that utilize the mechanical servo-drive technology. The mechanical servo-drive press offers the flexibility of a hydraulic press (infinite slide speed and position control, availability of press force at any slide position) with the speed accuracy and reliability of a mechanical press [14]. The new servo-drive presses can satisfy the requirement of implement VBHF simultaneously with VPV and stepwise motion of the servo-flexible stamping. So it can be predicted that the new servo-flexible stamping will become a new potential stamping process in the future.

5 Conclusions

Based on the plastic theory and correlative energy conservation theorem, a new theoretical mathematic model of VBHF had been established during the warm deep-drawing of TRC magnesium sheet. The results of experiments suggested that

the calculated load curve of minimum wrinkles VBHF using the new equation fit to the tested data very well. Furthermore, the warm deep-drawing results revealed that the LDR of cylinder parts was improved from 1.75 to 1.92 by the three segments way of loading VBHF, at the forming temperature of 523 K and punch velocity of 45 mm/min.

The numerical simulations indicated that the LDR can be improved observably from 1.86 to 2.26, and gained the whole cylinder part, by the new servo-flexible stamping technology that the three segments way of loading VBHF combined VPV.

References

1. Stanford N, Barnett M (2008) Effect of composition on the texture and deformation behaviour of wrought Mg alloys. *Scripta Mater* 58(3):179–182
2. Jiang J, Godfrey A, Liu W et al (2008) Identification and analysis of twinning variants during compression of a Mg–Al–Zn alloy. *Scripta Mater* 58:122–125
3. Wu L, Jain A, Brown DW et al (2008) Twinning-detwinning behavior during the strain-controlled low-cycle fatigue testing of a wrought magnesium alloy, ZK60A. *Acta Mater* 56(4):688–695
4. Chen FK, Huang TB, Chang CK (2003) Deep drawing of square cups with magnesium alloy AZ31 sheets. *Int J Mach Tools Manuf* 43(15):1553–1559
5. Zhang SH, Zhang K, Xu YC et al (2007) Deep-drawing of magnesium alloy sheets at warm temperatures. *J Mater Process Technol* 185(1–3):147–151
6. Doege E, Sommer N (1987) Blank-holder pressure and blank-holder layout in deep drawing of thin sheet metal. *Adv Technol Plast* 11:1305–1314
7. Yoshihara S, Manabe K, Nishimura H (2005) Effect of blank holder force control in deep-drawing process of magnesium alloy sheet. *J Mater Process Technol* 170(3):579–585
8. Doege E, Elend LE (2001) Design and application of pliable blank holder systems for the optimization of process conditions in sheet metal forming. *J Mater Process Technol* 111:182–187
9. Sheng ZQ, Jirathearanat S, Altan T (2004) Adaptive FEM simulation for prediction of variable blank holder force in conical cup drawing. *Int J Mach Tools Manuf* 44:487–494
10. Liang B, Hu S (1987) The plasticity theory of sheet forming. Mechanics Industry Press, Beijing (in Chinese)
11. Chang Qun-Feng, Li Da-Yong, Peng Ying-Hong (2007) Experimental and numerical study of warm deep drawing of AZ31 magnesium alloy sheet. *Int J Mach Tools Manuf* 47:436–443
12. Liu Z, Xing S, Bao P-W (2010) Characteristics of hot tensile deformation and microstructure evolution of twin-roll cast AZ31B magnesium alloys. *Trans Nonferr Met Soc China* 20:776–782
13. Liu Zhimin, Xingy Shuming, Bao Peiwei (2010) A new analytical model for the flow stress of twin-roll casting magnesium sheet at elevated temperatures. *J Mater Sci Technol* 26(5):461–466
14. Osakada K, Mori K, Altan T (2011) Mechanical servo press technology for metal forming. *CIRP Ann-Manuf Technol* 60:651–672

Proceedings of the FISITA 2012 World Automotive
Congress

Volume 11: Advanced Vehicle Manufacturing
Technology

; (Eds.)

2013, VIII, 249 p., Hardcover

ISBN: 978-3-642-33746-8